

# 2D isotropic negative permeability in a $\Lambda$ -type three-level atomic system\*

Shuang-Ying Zhang,<sup>1,†</sup> Shun-Cai Zhao<sup>ib,1,†</sup> and Ai-Ling Gong<sup>1</sup>

<sup>1</sup>*Faculty of science, Kunming University of Science and Technology, Kunming, 650093, PR China*

A approach for two-dimensional(2D) negative permeability in a  $\Lambda$ -type three-level atomic system interacting with a probe magnetic and the superposition of two orthogonal standing-wave fields is proposed. Through the theoretical analysis and numerical simulation, two equally and tunable peak maxima of negative magnetic responses are observed in the x-y plane, and around the peak maxima region the negative permeability is isotropic. A new avenue to 2D isotropic negative permeability in isotropic applications via quantum optics method is achieved in our schme.

PACS: 42.50.Gy ; 32.10.Dk ; 78.20.Cip

## I. INTRODUCTION

The artificial metamaterials[1] with simultaneously negative electric permittivity and magnetic permeability are called left-handed materials (LHMs). LHMs have attracted more and more attention[2, 3] because of their surprising and counterintuitive electromagnetic and optical properties[4–6], such as subwavelength resolution, reverse Doppler effect and Cherenkov radiation, negative Goos-Hänchen shift, reversed circular Bragg phenomenon, and et.c. Up to now, several approaches have been carried out to realize LHMs in experiments, including artificial composite metamaterials [2], photonic crystal structure[7–9], chiral material[10, 11]. However, the left-handedness(LH) in these approaches based on spatially periodic structure is usually anisotropic and accompanies a large absorption.

In that case, photonic resonant materials[12–23] based on quantum optics were believed to the candidate of isotropic LH without absorption. With the help of the electromagnetically induced transparency (EIT) effect and the Lorentz-Lorenz local field effect, the dense gases of atoms can realize LH with low absorption, even zero absorption[17, 18]. However, the magnetic permeability  $\mu_r$  of photonic resonant materials is always close to the free space value[24] because the typical transition magnetic-dipole moments are smaller than transition electric dipole moments by a factor of the order of

the fine structure constant ( $\alpha \approx \frac{1}{137}$ )[12, 25, 26], thus the permeability  $\mu_r$  is difficult to get negative value.

In this literature, the aim of two-dimensional (2D) isotropic negative permeability in the dense atomic gases under proper conditions is implemented. Although several schemes[27–35] for 2D LHMs have been proposed recently, the proposed 2D LHMs are based on classical electromagnetic theory and limited by the spatially periodic structure of the medium. Here, we firstly explore the possibility of implementing 2D negative magnetic effect based on quantum optics with two orthogonal standing-wave fields via density matrix theory depicting the interaction of light with matter semiclassically. And the orthogonal standing-wave field is obtained from the superposition of the two standing-wave fields along the x and y directions, respectively.

## II. THEORETICAL MODEL AND APPROACH

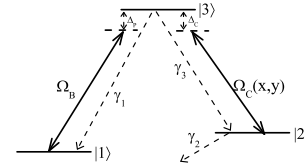


FIG. 1. Schematic diagram of a three-level atomic system. The magnetic-dipole transition  $|1\rangle \leftrightarrow |3\rangle$  is excited by probe magnetic field ( $\mathbf{B}$ ) with Rabi frequency  $\Omega_B$ . The transition from  $|2\rangle \leftrightarrow |3\rangle$  is driven by two superposition standing-wave fields with Rabi frequency  $\Omega_C(x, y)$ , which are along the x and y directions, respectively.

\* Supported by National Natural Science Foundation of China (NSFC) (Grant No.61205205) and the Foundation for Personnel training projects of Yunnan Province(grant No.KKSY201207068) of China.

† Corresponding author: zhaosc@kmust.edu.cn.

We consider a  $\Lambda$ -type three-level atom having an up-

per energy level  $|3\rangle$  and two closely lying lower energy levels  $|1\rangle$  and  $|2\rangle$ , showed in Fig.1. The magnetic-dipole transition  $|1\rangle \leftrightarrow |3\rangle$  is excited by the magnetic component of a probe magnetic field  $\mathbf{B}$  with frequency  $\nu_B$  and Rabi frequency of  $\Omega_B = \mathbf{B}\mu_{31}/2\hbar$ , where  $\mu_{31}$  is the corresponding magnetic dipole moment (magnetic-dipole matrix element). A standing-wave field  $\mathbf{E}(x, y)$  with frequency  $\nu_c$  and Rabi frequency  $\Omega_c(x, y)$  drives the transition  $|3\rangle \leftrightarrow |2\rangle$ . And the standing-wave field  $\mathbf{E}(x, y)$  is the superposition of two orthogonal standing-wave fields, i.e., one is in the x direction and the second is along y direction. However, each of the standing-wave fields is again the superposition of two standing-wave fields along the corresponding directions[36]. Note that the parity of level  $|2\rangle$  is different from those of  $|1\rangle$  and  $|3\rangle$ , so the level pairs  $|1\rangle \leftrightarrow |3\rangle$  and  $|2\rangle \leftrightarrow |3\rangle$  can be coupled to the probe magnetic field and the control electric field, respectively.  $\gamma_2$  and  $\gamma_3$  denote spontaneous emission decay rates and  $\gamma_1$  the collisional dephasing rate.  $\Delta_P$  and  $\Delta_C$  is frequency detuning corresponding to the probe magnetic field and standing-wave field, respectively.

In experimental investigation, the sample of metallic alkali atoms (e.g. Na, K, Rb) might be a good candidate for our scheme. Because the physical realizations for  $\{|1\rangle, |2\rangle, |3\rangle\}$  of the three-level system could be  $\{3^2S_{1/2}, 3^2P_{1/2}, 4^2S_{1/2}\}$  in neutral Na [22, 23]. It should be noted that here the atoms are assumed to be nearly stationary and hence any Doppler shift is neglected. To discuss the steady case of the optical properties of the atomic vapor, we calculate its magnetic permeability in two-dimensional x-y plane.

According to Schrödinger equation, the equation of motion of the off-diagonal density matrix elements of the atomic system are given as follows

$$\begin{aligned} \dot{\rho}_{31} = & i(\rho_{11} - \rho_{33})\Omega_B + i\rho_{21}\Omega_C(x, y) \\ & - \rho_{31}\left(\frac{1}{2}(\gamma_3 + \gamma_1) + i\Delta_P\right), \end{aligned} \quad (1)$$

$$\begin{aligned} \dot{\rho}_{21} = & -i\rho_{23}\Omega_B + i\rho_{31}\Omega_C^*(x, y) \\ & - \rho_{21}\left(\frac{\gamma_2}{2} + i(\Delta_P - \Delta_C)\right), \end{aligned} \quad (2)$$

$$\begin{aligned} \dot{\rho}_{32} = & i\rho_{12}\Omega_B + i(\rho_{22} - \rho_{33})\Omega_C(x, y) \\ & - \rho_{32}\left[\frac{1}{2}(\gamma_2 + \gamma_3 + \gamma_1) + i\Delta_C\right], \end{aligned} \quad (3)$$

In the steady state case, all the atoms remain in the ground and the atomic population in level  $|1\rangle$  is close

to unity. Thus we obtain

$$\rho_{11} = 1, \rho_{22} = 0, \rho_{33} = 0. \quad (4)$$

This set of equations can be solved, for example, by writing the matrix form,

$$\dot{\mathbf{R}} = -\mathbf{M}\mathbf{R} + \mathbf{A} \quad (5)$$

with

$$\begin{aligned} \mathbf{R} = & \begin{pmatrix} \rho_{31} \\ \rho_{21} \end{pmatrix}, \mathbf{A} = \begin{pmatrix} i\Omega_B \\ 0 \end{pmatrix}, \\ \mathbf{M} = & \begin{pmatrix} i\Delta_P + (\gamma_1 + \gamma_3)/2 & -i\Omega_C(x, y) \\ -i\Omega_C^*(x, y) & i(\Delta_P - \Delta_C) + \gamma_2/2 \end{pmatrix}. \end{aligned} \quad (6)$$

The solution of matrix Eqs.5 yields the steady solution as follows:

$$\begin{aligned} \rho_{31} = & \frac{i\Omega_B\xi}{\Omega_C(x, y)\Omega_C^*(x, y) + \xi\left(\frac{\gamma_3 + \gamma_1}{2} + i\Delta_P\right)}, \\ \rho_{21} = & \frac{-\Omega_B\Omega_C^*(x, y)}{\Omega_C(x, y)\Omega_C^*(x, y) + \xi\left(\frac{\gamma_3 + \gamma_1}{2} + i\Delta_P\right)}. \end{aligned} \quad (7)$$

where

$$\xi = \frac{\gamma_2}{2} + i(\Delta_P - \Delta_C).$$

The atomic magnetic polarizability associated with the optical transition  $|1\rangle \leftrightarrow |3\rangle$  is

$$\chi = \frac{2\mu_0\mu_{31}\rho_{31}}{B}. \quad (8)$$

According to the Clausius-Mossotti relation, the relative magnetic permeability of the atomic media be given by

$$\mu_r = \frac{1 + \frac{2}{3}N\chi}{1 - \frac{N\chi}{3}}, \quad (9)$$

where N is the atom number density. We set some typical parameters  $\gamma_1 = 0.5\gamma\text{Hz}$ ,  $\gamma_3 = 1.5\gamma\text{Hz}$ ,  $\gamma_2 = \gamma\text{Hz}$ . All the parameters are reduced to dimensionless units by scaling with  $\gamma$ , where  $\gamma = 10^7$ . The Rabi frequency of the standing-wave field is set in the form

$$\Omega_C(x, y) = \Omega_{C0}[\sin(kx + \phi) + \sin(ky + \varphi)], \quad (10)$$

where  $k = \frac{2\pi}{\lambda}$  is wave vector and wavelength is  $\lambda = 4\mu\text{m}$ . Other parameters are taken with  $\mu_{31} = 6.6 \times 10^{23}\text{Cm}^2\text{Hz}$ ,  $\Omega_{C0} = 5\gamma$  and atomic concentration  $N = 5.0 \times 10^{24}\text{m}^{-3}$ [22].

### III. RESULTS AND DISCUSSIONS

In the preceding sections, we calculate the relative magnetic permeability in present atomic vapor system. In what follows, let us discuss its optical properties by simulating the magnetic permeability. The behaviors of the magnetic permeability corresponding to the frequency detunings and the initial phases will be of interest.

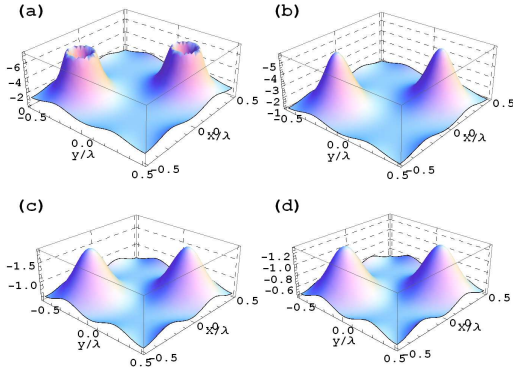


FIG. 2. (Color online) Plots for the 2D real part of magnetic permeability  $\text{Re}[\mu_r]$ :  $\text{Re}[\mu_r]$  versus  $x$  and  $y$  for different values of probe magnetic detunings  $\Delta_p$  (a) $\Delta_p=-2.5\gamma$ , (b) $\Delta_p=-4.1\gamma$ , (c) $\Delta_p=-7.5\gamma$ , (d) $\Delta_p=-9\gamma$ . And the initial phases  $\phi=0$ ,  $\varphi=0$  and  $\Delta_c=6.3\gamma$  were taken.

The calculated real parts of magnetic permeability  $\text{Re}[\mu_r]$  for different probe detuning parameters  $\Delta_p$  are shown in Fig.2 in a three-dimensional Cartesian coordinate system. The behavior of negative magnetic response is strong when the probe detunings are set  $-2.5\gamma$ ,  $-4.1\gamma$ ,  $-7.5\gamma$  and  $-9\gamma$  in Fig.2(a), (b), (c) and (d), respectively. As shown in Fig.2(a), two circular crater-like patterns with the peak maxima being about  $-6$  locate in the quadrants I and III. However, the peak patterns of  $\text{Re}[\mu_r]$  change into two circular spike-like patterns with their values being about  $-5$  in Fig.2(b). And the peak values of the two circular spike-like patterns collapse to  $-2$  when the value of  $\Delta_p$  is tuned to  $7.5\gamma$  in Fig.2(c). The peak values of the two circular spike-like patterns continue to decrease to  $-1.2$  when  $\Delta_p$  is set to  $-9\gamma$  in Fig.2(d). We noted the circular distribution of  $\text{Re}[\mu_r]$  has the same value circling around the center of the crater-like or spike-like patterns in Fig.2(a), (b), (c) and (d). The circular equivalent distribution shows the isotropic  $\text{Re}[\mu_r]$  in the

$x$ - $y$  plane.

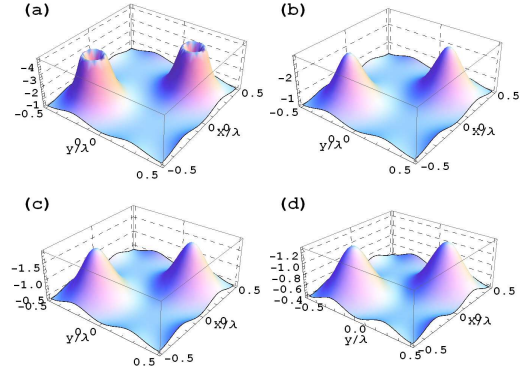


FIG. 3. (Color online) Plots for the 2D real part of magnetic permeability  $\text{Re}[\mu_r]$ :  $\text{Re}[\mu_r]$  versus  $x$  and  $y$  for different values of the standing-wave field detuning  $\Delta_c$ . (a) $\Delta_c=-4.5\gamma$ , (b) $\Delta_c=-1.9\gamma$ , (c)  $\Delta_c=0.2\gamma$ , (d) $\Delta_c=3.5\gamma$ .  $\Delta_p=-10\gamma$ , and all other parameters are the same as those in Fig.2.

Another tunable parameter is the coupling standing-wave fields detuning  $\Delta_c$  from the transition  $|2\rangle \leftrightarrow |3\rangle$ , and the corresponding 2D plots are shown in Fig.3. In Fig.3, the values of the standing-wave fields detunings  $\Delta_c$  equal to (a)  $-4.5\gamma$ , (b)  $-1.9\gamma$ , (c)  $0.2\gamma$ , and (d)  $3.5\gamma$ . Comparing with Fig.2, the behavior of negative magnetic response is relatively weak via the tuning detuning  $\Delta_c$ . The peak maxima in the center of quadrants I and III changes with not only the pattern but also the values. Two circular crater-like patterns with their peak values being  $-4$  when  $\Delta_c$  is tuned to  $-4.5\gamma$  in Fig.3(a). The circular crater-like patterns transform rapidly into the circular spike-like patterns in Fig.3 from (b) to (d), and their peak values show a downward trend, i.e., from  $-2.6$ ,  $-1.8$ , to  $-1.2$ . It's also noted that the peaks of  $\text{Re}[\mu_r]$  are circular distribution around their centers from the crater-like or spike-like patterns. The circular distribution of  $\text{Re}[\mu_r]$  shows the isotropy of  $\text{Re}[\mu_r]$  in the  $x$ - $y$  plane.

In the follows, the behavior of  $\text{Re}[\mu_r]$  dependent different initial phases is discussed in Fig.4(a) and (b). Fig.4 (c) and (d) are the contour plots corresponding to Fig.4(a) and (b), respectively. In Fig.4 (a), the initial phases for the standing-wave field are set  $\phi=0$ ,  $\varphi=0$  against  $\phi=-\pi$ ,  $\varphi=0$  in Fig.4 (b). We noticed that the amplitude ranges of  $\text{Re}[\mu_r]$  both are  $[-0.4, -1.0]$  and the two spike-like distribution graphs remain the same in Fig.4(a) and (b). The difference tuned by  $\phi$  between Fig.4(a) and

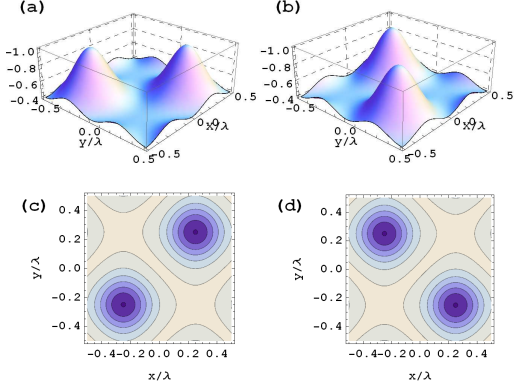


FIG. 4. (Color online) Plots for the 2D real part of magnetic permeability  $\text{Re}[\mu_r]$ :  $\text{Re}[\mu_r]$  versus  $x$  and  $y$  for different initial phases. (a)  $\phi=0$ , (b)  $\phi=-\pi$ , and their corresponding contour plots shown in (c), (d).  $\Delta_p=-10\gamma$ ,  $\Delta_c=7.2\gamma$ , all other parameters are the same as those in Fig.2.

(b) is the position. The positions of the two spike-like distribution graphs are in quadrants I and III in Fig.4(a) when  $\phi=0$ , while the positions change to quadrants II and IV when  $\phi=-\pi$  in Fig.4(b). The variation in positions is also displayed by their corresponding contour plots in Fig.4 (c) and (d), respectively. The contour plots corresponding to the two spike-like distribution graphs are concentric circles shown by Fig.4 (c) and (d). Taking the circle center as center, all of the values of  $\text{Re}[\mu_r]$  on the concentric circles are the same. The same values of  $\text{Re}[\mu_r]$  in the directions of  $360^\circ$  demonstrate the isotropy. So, an isotropic and homogeneous negatively permeability is ob-

tained in this atomic system. And the  $\Lambda$ -type three-level atomic system maybe particularly essential for designing devices such as a sub-wavelength focusing system or negative-index super-lens for perfect imaging.

#### IV. CONCLUSION

In conclusion, we presented a theoretical scheme for 2D isotropic negative permeability in the dense atomic gas via two orthogonal standing-wave fields. By adjusting the detunings corresponding to the probe and two orthogonal standing-wave fields, the flexible control negative magnetic responses are observed in the  $x$ - $y$  plane, and around the center of the circular crater-like or spike-like patterns  $\text{Re}[\mu_r]$  has the same value, which demonstrates the isotropic  $\text{Re}[\mu_r]$ . When the initial phases in the standing-field are manipulated, the positions of peak changes from quadrants I and III to quadrants II and IV, and their contour plots demonstrate clearly the isotropic and homogeneous  $\text{Re}[\mu_r]$ . The atomic vapor system in our scheme could be the candidate for 2D negative permeability and be a new avenue to 2D negative refraction research. Compared to other proposal, the atomic vapor scheme can eliminate some manufacturing constraints as well as reducing experimental difficulties. And we hope our scheme for 2D isotropic negative permeability could be achieved in the coming atomic medium experimentally.

- 
- [1] V. G. Veselago, *Sov.Phys.Usp* **10**(1968) 509.  
[2] J. B. Pendry, *Phys.Rev.Lett.* **85** (2000)3966.  
[3] R. A. Shelby, D. R. Smith, S. Schultz, *Science* **292** (2001) 77.  
[4] A. Lakhtakia, *Opt.Express* **11** (2003) 716.  
[5] A. Lakhtakia, *Int. J. Electron. Commun.* **58** (2004) 229.  
[6] L. Chen, S. He, L. F. Shen, *Phys. Rev. Lett.* **92** (2004) 107404.  
[7] P. V. Parimi et al., *Phys. Rev. Lett.* **92**( 2004) 27401.  
[8] A. Berrier et al., *Phys. Rev. Lett.* **93** (2004) 073902.  
[9] Z. Lu et al., *Phys. Rev. Lett.* **95** (2005)153901.  
[10] J. B. Pendry, *Science* **306** (2004)1353.  
[11] V. Yannopoulos, *J.Phys.: Condens. Matter* **18** (2006,)6883.  
[12] M. ö. Oktel, ö. E. Müteçaplğu, *Phys.Rev.A* **70**(2004)053806.  
[13] Q. Thommen, P. Mandel, *Phys. Rev. Lett.* **96** (2006) 053601.  
[14] J. Q. Shen, *Phys. Lett. A* **357** (2006) 54.  
[15] S. C. Zhao, *JETP Lett.* **94** (2011)347.  
[16] S. C. Zhao, *Sci China-Phys Mech Astron* **55** (2012) 213.  
[17] J. Kästel, M. Fleischhauer, *Phys. Rev. A* **79** (2009) 063818.  
[18] S. C. Zhao, Z. D. Liu, Q. X. Wu. *Opt. Commun.* **283** (2010) 3301.  
[19] J. Q. Shen, *J. Modern Opt.* **53** (2006) 2195.  
[20] J. Q. Shen, J. Almlöf, S. He, *Appl. Phys. A* **87** (2007) 291.

- [21] X. M. Su, H. X. Kang, J. Kou, X. Z. Guo, and J. Y. Gao, *Phys. Rev. A* **80** (2009) 023805.
- [22] J. Q. Shen, J. Almlöf, S. He, *Appl. Phys. A* **87** (2007) 291.
- [23] J. Q. Shen, *Prog. Theor. Exp. Phys.* **18** (2014) 033A01.
- [24] L. D. Landau, E. M. Lifshitz, and L. P. Pitaevskii, *Electrodynamics of Continuous Media* (Butterworth Heinemann, Oxford, 1998).
- [25] S. C. Zhao, Z. D. Liu, J. Zheng and G. Li, *Chin. Phys. B* **20** (2011)067802.
- [26] J. Kästel, M. Fleischhauer, S. F. Yelin, and R. L. Walsworth, *Phys. Rev. Lett.* **99** (2007) 073602.
- [27] A. Grbic and G. V. Eleftheriades, *IEEE transactions on antennas and propagation* **51** (2003) 2604.
- [28] T. Ueda, A. Lai and T. Itoh, *IEEE transactions on microwave theory and techniques* **55** (2007)1280.
- [29] A. Vallecchi, F. Capolino and A. G. Schuchinsky, *IEEE microwave and wireless components letters* **19** (2009) 5.
- [30] R. Islam, M. Zedler and G. V. Eleftheriades, *IEEE transactions on antennas and propagation* **59** (2011) 5.
- [31] M. Loncar, A. Scherer and Y. M. Qiu, *Appl. Phys. Lett.* **82**(2003)4648.
- [32] E. Cubukcu, *Nature* **423** (2003) 604.
- [33] R. Mindy, R. Lee and P. M. Fauchet, *Opt. Exp.* **15** (2007)4530.
- [34] D. Dorfner, T. Hürlimann, T. Zabel, G. Abstreiter, L. H. Frandsen and J. Finley, *Appl. Phys. Lett.* **93** (2008)181103.
- [35] F. Ouerghi, F. AbdelMalek, S. Haxha, E. K. Akowuah and H. Ademgil, *J. Light wave technology* **30** (2012) 3288.
- [36] B. K. Dutta, P. Panchadhyayee and P. K. Mahapatra, *Laser Phys.* **23** (2013) 045201.